PHYSICAL REVIEW B **70**, 180406(R) (2004)

# Density functional determination of the magnetic state of $\beta$-MnAs

Manish K. Niranjan, B. R. Sahu, and Leonard Kleinman
*Department of Physics, University of Texas at Austin, Austin, Texas 78712-0264, USA*

(Received 22 July 2004; published 29 November 2004)

Ferromagnetic hexagonal $\alpha$-MnAs has a first-order phase transition to $\beta$-MnAs at about 40 °C. Because it shows no long-range antiferromagnetic order, most workers assume that it is paramagnetic in spite of the fact that it does not have a Curie-Weiss magnetic susceptibility. With the aid of density functional calculations, we show that it is antiferromagnetic and explain the lack of observed long-range order.

DOI: 10.1103/PhysRevB.70.180406 PACS number(s): 75.50.Ee, 71.20.Be, 71.15.Nc

## I. INTRODUCTION

$\alpha$-MnAs was studied 100 years ago[1] and found to be ferromagnetic seven years later.[2] There has been recent renewed interest in MnAs because of its possible spintronic applications. Ramsteiner *et al.*[3] have studied spin injection from MnAs layers into GaAs while Tanaka *et al.*[4,5] have measured the epitaxial orientation and magnetic properties of MnAs thin films grown on GaAs. Although we know of no calculations of $\beta$-MnAs, there are three calculations[6–8] of the properties of zinc-blende MnAs, a phase which has never been grown and which was shown[7] could not be stabilized either by lattice stretching or compression.

More interesting to us is the $\beta$ phase, which is not ferromagnetic and which experiment has suggested is neither paramagnetic or antiferromagnetic. The transition from the hexagonal NiAs (space-group number 194) $\alpha$ phase to the orthorhombic MnP (space-group number 62) $\beta$ phase is first order and occurs at 40 °C (Ref. 9) or 44 °C (Ref. 10), the difference probably resulting from slightly different sample stoichiometries. Extrapolation of the magnetization versus temperature curve gives a Curie temperature[11] for the $\alpha$ phase of about 127 °C. The resistivity of the $\beta$ phase at 100 °C is about 3.3 times that of $\alpha$ phase at 35 °C.[12,13] Ney *et al.*[14] have found that the $\alpha$ and $\beta$ phases coexist between 10 and 40 °C in heteroepitaxially constrained MnAs/GaAs(001) films. The fact that $\beta$-NiAs transforms to the paramagnetic $\gamma$ phase (with the same NiAs structure as the $\alpha$ phase) at 130 °C, essentially the extrapolated Curie temperature of the $\alpha$ phase, together with the anomalous behavior of the inverse susceptibility of the $\beta$ phase, led Guillaud[13] to speculate that $\beta$-MnAs is antiferromagnetic. However, no long-range magnetic order has been detected by neutron diffraction.[9,15] Unlike $\beta$-MnAs, $\gamma$-MnAs shows normal Curie-Weiss behavior.[13]

There have been three different explanations for the $\alpha$ to $\beta$ transition. Kittel[16] proposed two ferromagnetic sublattices whose exchange coupling changed sign at the transition temperature leading to a ferromagnetic-antiferromagnetic transition. This theory was rejected by Goodenough and Kafalas[11] because no antiferromagnetic order had been observed. Rodbel *et al.*[17,18] purported to show with theory and experiment that the transition was ferromagnetic to paramagnetic. Their theory showed how such a phase transition could be first order in a very compressible material with a strongly volume-dependent exchange interaction. The $\alpha \rightarrow \beta$ transition with increasing pressure has been measured by others[11] as has the $\beta$ to $\alpha$ transition with increasing magnetic field.[10,19] Goodenough[11,20] pointed out how the $\alpha$ to $\beta$ and $\beta$ to $\gamma$ transition could be explained by a high spin Mn configuration in the $\alpha$ and $\gamma$ phases and a low spin Mn configuration in the $\beta$ phase. Andresen *et al.*[21] found a spiral density wave in $\beta$-MnAs. They worked at 4.2 and 80 K without stating whether it was present at both temperatures. The $\beta$ phase, created with 12.6 kbar of pressure, remains metastable below 160 K at 1 bar. The $\beta$ phase can also be stabilized by substituting a small amount of V, Cr, Fe, Co, or Ni for the Mn, or P for the As, resulting in a Néel temperature of 200-230 K. Thus, it is unlikely (especially since it has never been observed) that $\beta$-MnAs above 40 °C would support a spiral spin-density wave. We now restate the facts concerning the $\beta$ phase and then give the only description of the $\beta$ phase consistent with these facts and with Occam's razor. $\beta$-MnAs is not ferromagnetic. It is unlikely to be paramagnetic because it does not have Curie or Curie-Weiss behavior. Unlike the $\alpha$ to $\beta$ transition, Jahn-Teller structurally driven phase transitions go from lower to higher symmetry with increasing temperature. Thus, except for the fact that no antiferromagnetic order has been seen in the $\beta$ phase, this transition would seem to be magnetically driven, from the high symmetry ferromagnetic state to a lower symmetry antiferromagnetic state. Our solution to this conundrum is that $\beta$-MnAs consists of antiferromagnetic planes of Mn but that the exchange coupling between planes is so weak that the ordering of the planes is random, i.e., an up spin in one plane is equally likely to be below an up or a down spin in the plane above. This randomness accounts for the failure of neutron scattering to detect long-range antiferromagnetic order. In the next section we show that this description is consistent with the results of density functional calculations.

## II. CALCULATIONS AND RESULTS

These ultrasoft pseudopotential[22] calculations were done using the PWSCF package of Baroni *et al.*[23] We sampled a $12\times12\times8$ **k**-point mesh in the hexagonal Brillouin zone (cf. $3\times3\times3$ in Ref. 7) and a $12\times8\times8$ in the orthorhombic. The PBE (Ref. 24) exchange-correlation density functional was used and plane waves up to 35 Ry were used in the expansion. The partial core correction[25] was used on the As atoms, but, in lieu of one on Mn, the Mn $3s$ and $3p$ semicore

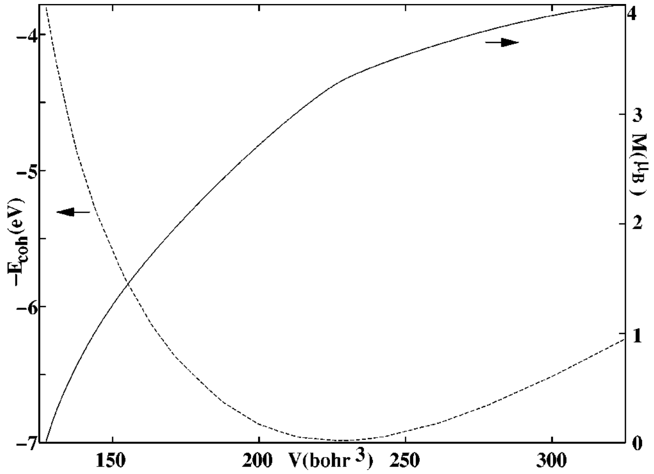

FIG. 1. Magnetization of $\alpha$-MnAs in bohr magnetons per MnAs (solid line) and negative of the cohesive energy per MnAs in eV (dashed line) as a function of volume.

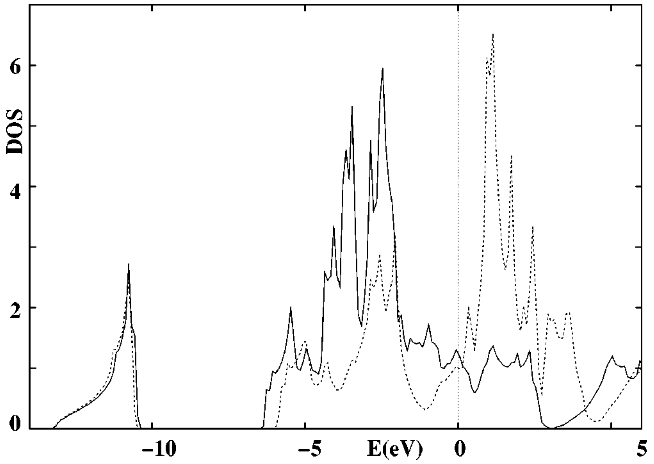

FIG. 2. Majority (solid line) and minority spin (dashed line) densities of states in electrons per eV per unit cell of $\alpha$-MnAs. The Fermi energy is at $E=0$.

states were included in the calculations. The hexagonal calculations were converged to $10^{-8}$ Ry while the orthorhombic calculations were converged to $10^{-5}$ Ry. The orthorhombic lattice constants and atomic displacements were calculated starting from the experimental values and iterating until all forces were less than 0.4 mRy/bohr and all stresses less than 0.22 mRy/bohr.[3]

A plot of minus the cohesive energy (obtained by subtracting the energy of spin-polarized atoms from the total energy) and the magnetization of $\alpha$-MnAs versus volume is displayed in Fig. 1. One sees that it requires about a 47% reduction in the volume from its equilibrium value to cause the magnetization to disappear in what appears to be a second-order phase transition. Although there would be a transition to the $\beta$ phase before this occurred, the volume-dependent magnetization theory of Rodbell *et al.*[17,18] does not require a structural transition. Because the $\beta$-phase volume is only 2% smaller[9] than the $\alpha$, it is highly unlikely that the theory of Rodbell *et al.* is applicable to the phase transition in MnAs. In Table I we compare the equilibrium volume, cohesive energy, $c/a$ ratio, bulk modulus, and magnetization with experiment for $\alpha$-MnAs. The volume and $c/a$ were measured[21] at 4.2 K. Our 0.96% discrepancy with the experimental volume is extremely small for a density functional calculation while our $c/a$ ratio is no better than fair agreement with experiment. The $c/a$ ratio decreased monotonically with volume from 1.76 at $V=254.5$ bohr$^3$ to 1.39 at $V=649.0$ bohr.$^3$ Because of the nonlinearity of the exchange-correlation potential, our excellent agreement with the experimental[11] magnetization might have been slightly worse had more core electrons been included in the calculation. Our zero-temperature bulk modulus seems not inconsistent with the 273-K experimental[26] value. We could find no experimental value for the cohesive energy, but our calculated cohesive energy is quite consistent with our bulk modulus. For example, scandium has a bulk modulus of 43.5 GPa (Ref. 27) and a cohesive energy of 7.8 eV (Ref. 27) per two atoms. Figure 2 is a plot of the spin density of states (DOS) at the calculated equilibrium volume. The split off low-energy states are the As 4*s* bands while the higher lying states come from the hybridizing As 4*p* and Mn 3*d* bands.

TABLE I. Equilibrium unit-cell volume (in bohr$^3$), cohesive energy (in eV per MnAs), $c/a$ ratio, magnetization (in bohr magnetons per Mn atom), and bulk modulus (in GPa) compared with experiment for $\alpha$-MnAs.

| | Vol | $E_{coh}$ | $c/a$ | $M$ | $B$ |
|---|---|---|---|---|---|
| Calc. | 456.21 | 6.982 | 1.488 | 3.32 | 44.5 |
| Expt. | 460.62[a] | | 1.519[a] | 3.4[b] | 35.8[c] |

[a] References 21.
[b] References 11.
[c] References 26.

The $\beta$-MnAs unit cell is obtained from the $\alpha$ by small distortions as follows. A hexagonal lattice has a centered rectangular unit cell with $b=\sqrt{3}a$ and twice the area. $b$ and $a$ each relax by about $-1$%, almost, but not quite, maintaining their $\sqrt{3}$ ratio, while $c$ does not relax at all.[9] Although the unit cell is almost hexagonal, there are sizable inner displacements of the atoms which destroy the almost hexagonal symmetry. We have defined $a$, $b$, and $c$ to be consistent with the hexagonal lattice. To get the standard definition used in Ref. 9 $(abc)\rightarrow(bca)$.

In Table II we list the cohesive energy and magnetization for ferromagnetic, paramagnetic, and three different antiferromagnetic structures of $\beta$-MnAs. The two (001) planes of

TABLE II. Cohesive energy (per MnAs) calculated at the experimental high-temperature lattice constants and inner displacements as well as with lattice constants and inner displacements relaxed to their equilibrium values for ferromagnetic, paramagnetic, and three antiferromagnetic structures described in text.

| | Ferro | Para | AFI | AFII | AFIII |
|---|---|---|---|---|---|
| Expt. | 6.973 | 5.998 | 6.880 | 6.909 | 6.904 |
| Rlx. | 6.982 | 6.507 | 6.896 | 6.936 | 6.937 |

TABLE III. Calculated orthorhombic lattice constants (in bohr), volume (in bohr$^3$), and magnetization (in bohr magnetons per MnAs) for the five crystals in Table II, compared with experimental values at 55 °C and 4.2 K with an applied pressure of 12.6 kbar. Note that $b=\sqrt{3}a$ for the ferromagnetic case which has hexagonal symmetry.

| | $a$ | $b$ | $c$ | $V$ | $M$ |
|---|---|---|---|---|---|
| Ferro. | 7.070 | 12.246 | 10.522 | 910.99 | 3.32 |
| Para. | 6.405 | 11.427 | 10.215 | 747.69 | 0.00 |
| AFI | 6.830 | 11.915 | 10.768 | 876.29 | 3.38 |
| AFII | 6.879 | 11.907 | 10.732 | 878.98 | 3.56 |
| AFIII | 6.866 | 11.888 | 10.716 | 874.73 | 3.40 |
| 55 °C[a] | 6.931 | 12.032 | 10.809 | 901.40 | |
| 4.2 K[b] | 6.603 | 11.641 | 10.547 | 810.70 | |

[a] Reference 9.

[b] Reference 21.

Mn are ferromagnetic but oppositely polarized in AFI. In AFII the planes are antiferromagnetic with up (down) spins in one plane below up (down) spins in the other, and in AFIII the down (up) spins are below the up (down). The results are listed for the fully relaxed positions as well as for the starting high-temperature[9] lattice constants and inner displacements which are listed in Tables III and IV. It is interesting to note that with the experimental lattice parameters the ferromagnetic state is still the ground state. It relaxes back to $\alpha$-MnAs. It is also interesting to note that in spite of their smaller volume, all three antiferromagnets appear to have a larger magnetization than the ferromagnet. This is because all ferromagnets of which we are aware have their magnetization reversed in their interstitial regions. Had we listed the integrated absolute value of the magnetization per Mn atom for the ferromagnetic case as we did for the antiferromagnetic, $M$ would have been $3.72\mu_B$. The paramagnetic crystal has by far the largest volume relaxation and thus the biggest increase in cohesive energy. Even so, its cohesive energy remains 430-meV below that of AFIII. Thus, there are three reasons to discard it as a possible candidate for $\beta$-MnAs above 40 °C: its small cohesive energy, its volume which is much smaller than experiment, and its unusual magnetic susceptibility.

TABLE IV. Calculated positions of the atoms within the unit cells of Table III compared with experiment at 55 °C. The Mn atoms are at $[\frac{1}{4},\frac{1}{4}-\alpha,-\beta]$, $[\frac{3}{4},\frac{3}{4}+\alpha,+\beta]$, $[\frac{3}{4},\frac{3}{4}-\alpha,\frac{1}{2}+\beta]$, $[\frac{1}{4},\frac{1}{4}+\alpha,\frac{1}{2}-\beta]$ and the As atoms are at $[\frac{1}{4},-\frac{1}{12}+\gamma,\frac{1}{4}+\delta]$, $[\frac{3}{4},\frac{1}{12}-\gamma,\frac{3}{4}-\delta]$, $[\frac{3}{4},\frac{5}{12}+\gamma,\frac{1}{4}-\delta]$, $[\frac{1}{4},\frac{7}{12}-\gamma,\frac{3}{4}+\delta]$.

| | $\alpha$ | $\beta$ | $\gamma$ | $\delta$ |
|---|---|---|---|---|
| Ferro. | 0 | 0 | 0 | 0 |
| Para. | 0.0528 | 0.0056 | 0.0069 | 0.0539 |
| AFI | 0.0100 | 0.0014 | 0.0001 | 0.0082 |
| AFII | 0.0475 | 0.0135 | 0.0049 | 0.0447 |
| AFIII | 0.0435 | 0.0030 | −0.0019 | 0.0444 |
| Exp[a] | 0.0271 | 0.0047 | 0.0020 | 0.0245 |

[a] Reference 9.

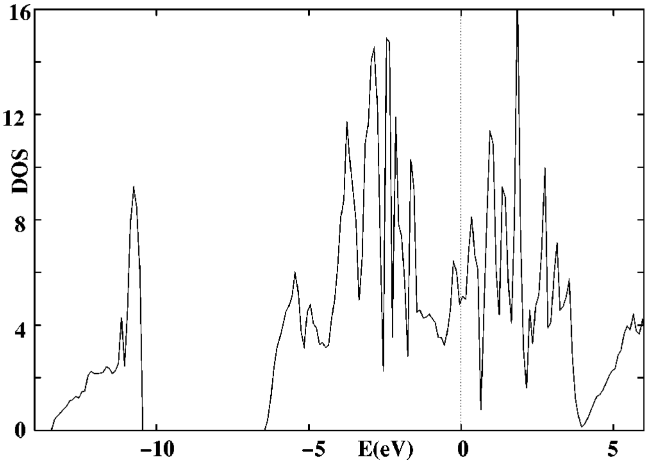

FIG. 3. Total density of states in electrons per eV per unit cell of $\beta$-MnAs. The Fermi energy is at $E=0$.

In Table III we note that the relaxed lattice constants of all three antiferromagnetic structures are smaller than the experimental values at 55 °C, as expected, but that they are larger than those measured at 4.2 K under 12.6 kbar of applied pressure while the paramagnetic lattice constants are much smaller than the experimental ones under 12.6 kbar. Table IV displays the displacements of the atoms in the orthorhombic structure away from their positions in the hexagonal structure. One peculiarity is that the atomic displacements of AFI away from hexagonal are much smaller than those of AFII and AFIII but its $b/a=1.745$ is much further from the hexagonal $\sqrt{3}$ than the 1.731 of both AFII and AFIII. Figure 3 is the DOS of AFIII. If we divide these in half (because the unit cell is twice as large) and compare them with the sum of spin DOS of Fig. 2, we see that at the Fermi energy the $\beta$-phase DOS is about 8% larger than the $\alpha$. Thus, the 3.3 times larger resistivity of the $\beta$ phase[12,13] must be due to other sources, such as the 65-K higher temperature at which it was measured, in addition to the postulated disorder of its antiferromagnetic planes.

## III. CONCLUSIONS

We believe that our calculation is sufficiently accurate to discard the possibility of $\beta$-MnAs being paramagnetic even without considering its non-Curie-Weiss magnetic susceptibility. Since it is not ferromagnetic, that leaves only the possibility of its being a planar antiferromagnet with planes randomly ordered to account for the lack of observed antiferromagnetic order or its being in some more complicated state that we have not considered. A spin glass seems highly unlikely for an ordered compound and a spin-density wave or spiral spin-density wave would have been detected by neutron scattering. The question then remains, how consistent is this random antiferromagnetic state with our calculations? We see that AFIII (aligned planes) and AFII (staggered planes) are degenerate, which makes it very likely that their free energies at 40 °C will be very close to degenerate and that rather than be staggered or aligned, the planes will be random. We found the random antiferromagnet state lies

40 meV below AFI with its alternating ferromagnetic planes. It also lies 45 meV above the hexagonal ferromagnetic state. The fact that the $\alpha-\beta$ transition occurs with increasing temperature indicates that there are contributions to the entropy which favor the antiferromagnetic $\beta$ phase over the ferromagnetic $\alpha$ phase.We can only speculate what these might be. The almost perfect hexagonal lattice symmetry indicates that the inner displacements of Table IV select 1 of 6 equivalent sets of atomic sites. If some of the energy barriers between these sites are small, they could cause there to be very low-frequency phonon modes in the $\beta$ phase which are not present in the $\alpha$ phase.[28] These, together with the uncertainties of density functional theory, should be sufficient to account for the 45 meV in the free energy needed to account for the transition to the disordered antiferromagnetic state. Therefore, we believe that our proposed disordered antiferromagnetic state is consistent with these calculations and is the most likely state for $\beta$-MnAs.

## ACKNOWLEDGMENTS

This work was supported by the Welch Foundation (Houston, TX) and Texas Advanced Computing Center(TACC), University of Texas at Austin.

---

[1] F. Heuser, Z. Angew. Chem. **17**, 260 (1904).

[2] S. Hilpertand and T. Dieckmann, Ber. Dtsch. Chem. Ges. A **44**, 2378 (1911).

[3] M. Ramsteiner, H. Y. Hao, A. Kawaharazuka, H. J. Zhu, M. Kastner, R. Hey, L. Daweritz, H. T. Grahn, and K. H. Ploog, Phys. Rev. B **66**, 081304(R) (2002).

[4] M. Tanaka, J. P. Harbison, M. C. Park, T. Shin, and G. M. Rothberg, T. Shin, Appl. Phys. Lett. **65**, 1964 (1994).

[5] M. Tanaka, K. Saito, M. Goto, and T. Nishmaga, J. Magn. Magn. Mater. **198-199**, 719 (1999).

[6] T. Ogawa, M. Shirai, N. Suzuki, and I. Kitagawa, J. Magn. Magn. Mater. **196-197**, 428 (1999).

[7] Stefano Sanvito and Nicola A. Hill, Phys. Rev. B **62**, 15 553 (2000).

[8] Yu-Jun Zhao, W. T. Geng, A. J. Freeman, and B. Delley, Phys. Rev. B **65**, 113202 (2002). Note that the $\alpha$ and $\beta$ phase notation in this paper is not standard.

[9] R. H. Wilson and J. S. Kasper, Acta Crystallogr. **17**, 95 (1964).

[10] F. Ishikawa, K. Koyama, K. Watanabe, and H. Wada, Jpn. J. Appl. Phys., Part 2 **42**, L918 (2003).

[11] J. B. Goodenough and J. A. Kafalas, Phys. Rev. **157**, 389 (1967).

[12] A. Serres, J. Phys. Radium **8**, 146 (1947).

[13] C. Guillaud, J. Phys. Radium **12**, 223 (1951).

[14] A. Ney, T. Hesjedal, C. Pampuch, A. K. Das, L. Daweritz, R. Koch, K. H. Ploog, T. Tolinski, J. Lindner, K. Lenz, and K. Baberschke, Phys. Rev. B **69**, 081306(R) (2004).

[15] G. E. Bacon and R. Street, Nature (London) **175**, 518 (1955).

[16] C. Kittel, Phys. Rev. **120**, 335 (1960).

[17] C. P. Bean and D. S. Rodbell, Phys. Rev. **126**, 104 (1962).

[18] R. W. De Blois and D. S Rodbell, Phys. Rev. **130**, 1347 (1963).

[19] J. Mira, F. Rivadulla, J. Rivas, A. Fondado, T. Guidi, R. Caciuffo, F. Carsughi, P. G. Radaellil, and J. B. Goodenough, Phys. Rev. Lett. **90**, 097203 (2003).

[20] J. B. Goodenough, M.I.T. Lincoln Laboratory, Lexington MA, Technical Report No. 345, DDC 435758, 1964 (unpublished).

[21] A. F. Andresen, H. Fjellvag, and B. Lebech, J. Magn. Magn. Mater. **43**, 158 (1984).

[22] David Vanderbilt, Phys. Rev. B **41**, R7892 (1990).

[23] S. Baroni, A. Dal Corso, S. de Gironcoli, and P. Giannozzi, http://www.pwscf.org

[24] J. P. Perdew, K. Burke, and M. Ernzerhof, Phys. Rev. Lett. **77**, 3865 (1996).

[25] S. G. Louie, S. Froyen, and M. L. Cohen, Phys. Rev. B **26**, 1738 (1982).

[26] *Handbook of Physical Quantities*, edited by Igor. S. Grigoriev and Evgenii Z. Meilikhov, (CRC Boca Raton, 1997).

[27] Charles Kittel, *Introduction to Solid State Physics*, 7th ed. (Wiley, New York, 1996).

[28] We know of no experimental or theoretical work to confirm or refute this speculation. A calculation to compare the phonon spectra of the two phases is possible, but the purpose of this paper is to determine the magnetic structure of the $\beta$-phase and not to find the cause of the $\alpha$ to $\beta$ transition.